PNAS Nexus, 2023, 2, 1–10
https://doi.org/10.1093/pnasnexus/pgad057
Advance access publication 14 March 2023
Research Report

Increase in grain production potential of China under climate change

Zhuoran Liang[a,1], Laixiang Sun[b,c,1], Zhan Tian[d,*], Günther Fischer[e] and Huimin Yan[f]

[a]Hangzhou Meteorological Service, Hangzhou, Zhejiang 310051, China
[b]Department of Geographical Sciences, University of Maryland, College Park, MD 20742, USA
[c]School of Finance and Management, SOAS University of London, London WC1H 0XG, UK
[d]School of Environmental Science and Engineering, Southern University of Science and Technology, Shenzhen, Guangdong 518055, China
[e]International Institute for Applied Systems Analysis (IIASA), Laxenburg A-2361, Austria
[f]Institute of Geographical Sciences and Natural Resources Research (IGSNRR), Chinese Academy of Sciences, Beijing 100101, China
*To whom correspondence should be addressed: Email: tianz@sustech.edu.cn (Z.T.)
[1]Joint first authors.
Edited By: Michael Ladisch

Abstract

The rapid growth of China's demand for grains is expected to continue in the coming decades, largely as a result of the increasing feed demand to produce protein-rich food. This leads to a great concern on future supply potentials of Chinese agriculture under climate change and the extent of China's dependence on world food markets. While the existing literature in both agronomy and climate economics indicates a dominance of the adverse impacts of climate change on rice, wheat, and maize yields, there is a lack of study to assess changes in multi-cropping opportunities induced by climate change. Multi-cropping benefits crop production by harvesting more than once per year from a given plot. To address this important gap, we established a procedure within the agro-ecological zones (AEZ) modeling framework to assess future spatial shifts of multi-cropping conditions. The assessment was based on an ensemble of five general circulation models under four representative concentration pathway scenarios in the phase five of coupled model inter-comparison project and accounted for the water scarcity constraints. The results show significant northward extensions of single-, double-, and triple-cropping zones in the future which would provide good opportunities for crop-rotation-based adaptation. The increasing multi-cropping opportunities would be able to boost the annual grain production potential by an average scale of 89(±49) Mt at the current irrigation efficiency and 143(±46) Mt at the modernized irrigation efficiency with improvement between the baseline (1981–2010) and the mid-21st century (2041–2070).

Keywords: climate change adaption, food security, multiple cropping, supply potentials, China

Significance Statement

Multiple cropping is regarded as key to agricultural intensification and diversification. Despite the rich knowledge on the practice of multiple cropping in the past, the future changes in multi-cropping systems driven by global warming has been poorly accounted for in the assessments of future food production. We establish a procedure within the agro-ecological zones modeling framework to assess future spatial shifts of multi-cropping conditions in China, the world's largest food producer and consumer. The results show significant northward extensions of single-, double-, and triple-cropping zones, and the resultant increase in annual grain production potentials by 89(±49) to 143(±46) Mt. A 66% utilization of the increased potential would safeguard China's food security and ease the pressure on the global food market in the future.

Harvesting two or more crops from a single plot within one year is termed multiple cropping, which has been a common practice in low-land tropical and subtropical agriculture where rainy seasons are long enough or irrigation is viable (1). It is a land-use management strategy aiming to maximize the use of agro-climatic resources such as capturing energy from solar radiation as well as heat and moisture provision under the prevailing technology and input level. In the case that more food needs to be produced using the given cropland, which is typical in many countries nowadays, increasing multi-cropping intensity is an effective way to boost total production of crops. For example, it was reported that between 1961 and 2007, increase in multiple cropping had contributed to 9% increase in global crop production (2); from 2003 to 2016, the implementation of double-cropping offset the equivalent of 76.7 million ha of Brazilian arable land for grain production (3); and from 1981 to 2010, the northward shifts of double- and

Competing Interest: The authors declare no competing interest.
Received: November 9, 2022. **Revised:** February 12, 2023. **Accepted:** February 14, 2023

triple-cropping zones in China resulted in a 2.2% increase in the total production of maize, wheat, and rice (4). It is also acknowledged that multiple cropping with diverse crop species allows for risk diversification to different growing seasons and different crops for own use or markets (1), with the crop-, location-, and management-specific downsides that growing a second or third crop can increase the risks of crop failure (5) and environmental degradation (6–8).

Despite the rich knowledge on the practice of multiple cropping in the past, the first-time mapping of existing multi-cropping systems on the global scale was completed in 2020 (1), and the future changes in multi-cropping systems driven by global warming has been poorly accounted for in the assessments of future food production. In the context of China, where nearly half of the cultivated land has been subject to multiple cropping practices (9), the scientific assessments of future food production have focused on yield changes affected by global warming. For example, Huang et al. (10) reported that a search of key words and research themes from Web of Science on 2019, January 18, obtained 1,245 articles on future yield changes in China published after 2007. We repeated this search by adding the key words "multiple cropping" and "multi-cropping" on 2022, June 11, and obtained only two articles (4, 11) which contained an assessment of the potential increases in multi-cropping opportunities and the associated impacts on the total grain production of China. Nevertheless, the assessments in these two publications have obvious weaknesses. First, both of them adopted one emission scenario of A1B from the IPCC Fourth Assessment (AR4). Second, one (4) adopted the regional climate change model of RegCM3 only and the other (11) the UK Met Office's Providing REgional Climate for Impacts Studies only. Third, both of them did not consider irrigation water constraints in the future. Fourth, there was a lack of formal rule to optimally determine the crop sequence in a given multi-cropping zone. While the first two weaknesses can be addressed by running the assessment with more climate models and emission scenarios, it is the difficulties in addressing the last two weaknesses that have prevented the advancement in assessing the potential contributions of future changes in multi-cropping systems to the total grain production in China and beyond.

In this study, we addressed all of the above four weaknesses and thus provided a rigorous and robust assessment of the future changes in China's multi-cropping systems and the associated contributions to the grain production potentials in the country. For this purpose, we established a procedure within the agro-ecological zones (AEZ) modeling framework (12) to assess future spatial shifts of multi-cropping conditions. The AEZ model is able to carry out a systematic and spatially detailed accounting and assembly of climatic elements which influence the suitability and productivity of crops. We run the assessment for an ensemble of five general circulation models (GCMs) under four representative concentration pathway (RCP) scenarios in the phase five of coupled model inter-comparison project (CMIP5), with 1981–2010 as the baseline and the 2050s (2041–2070) as the future period. In addition to use the standardized soil–plant–atmosphere interaction algorithms of the AEZ model, our assessment procedure considers the water scarcity constraints in a spatially explicit manner and includes a module to determine the optimal cropping sequence in each grid-cell of a multi-cropping zone.

Results

Increases in multi-cropping opportunities

The main results on spatial shifts of multi-cropping zones are presented in Fig. 1 and Table 1. Fig. 1 visualizes border shifts of the triple-cropping zone and limited double-cropping zone in current irrigated cropland under the ensemble of five GCMs driven by four RCP scenarios. It shows that the extents of the two multi-cropping classes will move northwards and/or northwest-wards from their baseline north/northwest borders to the 2050s' north/northwest borders. This shift would lead to significant increases in multi-cropping opportunities. The boxplots in Fig. 1 indicate that the triple-cropping areas will extend northward by as much as 8.17 Mha (median) or 9.32 Mha (mean); the double-cropping area (borders are shown on the map) will extend northwestward by 3.07 Mha (median) or 3.46 Mha (mean); and the extension of limited double-cropping areas toward northwest and northeast will amount to 5.59 Mha (median) and 5.38 Mha (mean).

Table 1 presents the transition matrix of the multi-cropping class extents between the baseline and the 2050s ensemble of 20 GCM-RCP scenarios. This matrix is a summary of grid-level results for respectively irrigated and rain-fed cropland. As is to be expected under global warming, the matrix for irrigated cropland shows a significant "one-way" transition from lower to higher multi-cropping classes. For example, as shown in the second row of the matrix, of the baseline total 9.63 Mha single cropping extent, 5.38 (±1.28) Mha will become suitable for limited double-cropping, 0.14 (±0.34) Mha for double-cropping, and 4.11 (±1.49) Mha remain in the same class. The sixth row of the matrix shows that the 7.3 (±1.12) Mha and 0.05 (±1.65) Mha of the baseline total 10.08 Mha limited triple-cropping areas will become fit for triple-cropping and triple rice cropping, respectively. Looking at the columns of the matrix, for example, the 11.15 Mha limited triple-cropping areas (sixth column) in the 2050s will come from the transition of areas classified in the baseline as double-cropping with rice (7.62 ± 1.12 Mha) and double-cropping (0.8 ± 1.36 Mha), plus 2.73 (±1.90) Mha remaining in the same class. In summary, the extents of triple rice, triple-cropping, limited triple-cropping, and limited double-cropping classes will increase from 3.71, 7.62, 10.08, and 6.64 Mha in the baseline to 6.36, 14.29, 11.15, and 7.64 Mha in the 2050s, respectively. Correspondingly, the extents of limited single, single, double, and double with rice classes will decrease from 0.38, 9.63, 9.00, and 12.88 Mha in the baseline to 0.18, 4.31, 4.60, and 10.25 Mha in the 2050s, respectively. The total extent of this upward transition amounts to 35.84 Mha.

Unlike the one-directional transition of irrigated cropland (indicated by the values above the diagonal elements), the matrix for rain-fed land shows a more complicated two-way transition with values both above and below the diagonal. However, summing up the respective values above (21.81 Mha) and below (4.75 Mha) the diagonal shows that transitions to a higher class are more than four times the transitions to a lower class. This means that under rain-fed conditions, the simulated climate changes in 2050s will very and likely lead to an increase in China's multi-cropping potential.

Increases in grain production potential

Fig. 2 reports the estimated increases in the total grain production potentials from the baseline (1981–2010) to the 2050s (2041–2070) at the current and the advanced irrigation efficiency rate on the existing cropland with the currently available irrigation water supply. The boxplots show that at the current irrigation efficiency level (0.565 ± 0.074) (13), the sum of these changes across all multi-cropping classes gives a total increase of cereal production potential by some 88.8 (±49.4) Mt compared to the baseline. Atthe advanced irrigation efficiency level of 0.8 (14, 15), the

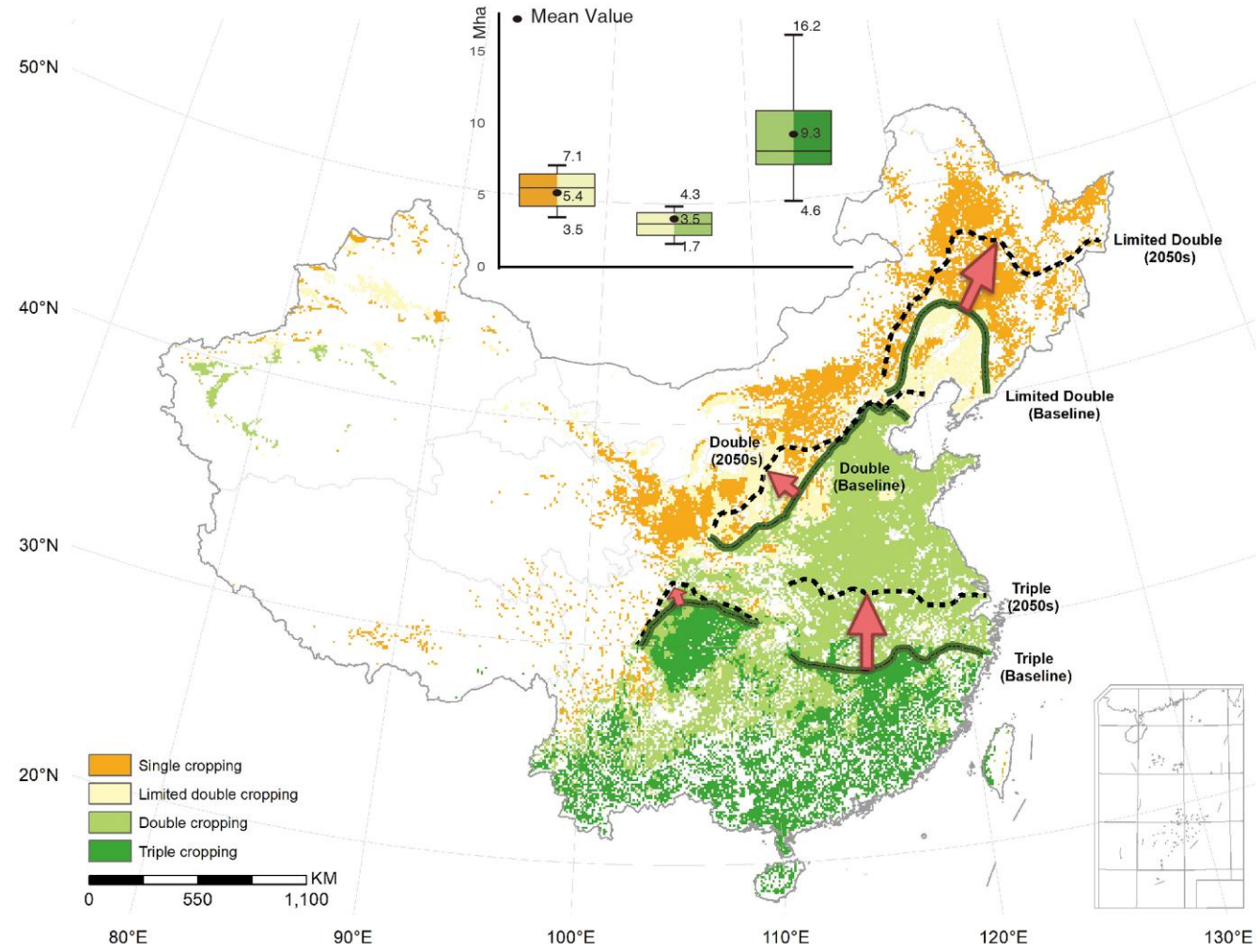

Fig. 1. Shifts of multi-cropping class extents in irrigated cropland from the baseline (1981–2010) to the 2050s (2041–2070) ensemble of 20 GCM-RCP simulations. Boxplots above the map show the distributions of the simulated shifting extents: the extended area of limited double into single cropping area in the baseline (left), the extended area of double-cropping into limited double area in the baseline (middle), and the extended area of triple-cropping into double-cropping area in the baseline (right).

corresponding total increase of cereal production potential would reach 143.1 (±46.4) Mt. If 66% of the increased potential could be utilized as reported in recent yield-gap analyses based on historical data in China (16, 17), an additional 58.6 (±32.6) Mt or 94.4 (±30.6) Mt cereal would be produced on the existing cropland at the current or advanced irrigation efficiency rate, respectively. These increases are equivalent to 89.6% (±49.8%) and 144.4% (±46.8%) of China's cereal imports (65.38 Mt) (18) in 2021, and 9.3% (±5.2%) and 14.9% (±4.8%) of China's cereal production (632.76 Mt) in the same year (19). While the increase at the current irrigation efficiency level seems moderate, the increase at the advanced irrigation efficiency rate would be able to bring China back to self-sufficiency in food supply in the future. This is an excellent news for both China and the world.

The Nightingale rose chart visualizes the variations across the 20 GCM-RCP simulations and highlights the significant contributions of the improvement in irrigation efficiency to the growth in cereal production potential. First, the growth in cereal production potential would take place under all of the 20 GCM-RCP scenarios. Second, at the current irrigation efficiency rate, the increases in cereal production potential under the MIROC-ESM-CHEM model driven by all four RCPs and the GFDL-ESM2M model driven by three RCPs except RCP8.5 are less than 5% of the baseline production potential. By contrast, achieving the advanced irrigation efficiency rate would drive the increases well above 6% of the baseline production potential under all 20 GCM-RCP combinations, above 10% under 12 GCM-RCP combinations, above 15% under six GCM-RCP combinations, and above 20% under the HadGEM2-ES and RCP8.5 combination. This means that the increase in cereal production potential will be robust and significant if modernized irrigation infrastructure can be phased in during the research period.

Keeping in mind the controversies surrounding the impact of CO_2 fertilization (20), Fig. S1 reports the parallel results which take the effect of CO_2 fertilization into account in a way as specified in the AEZ model (12). Because the maximum yield increment attributed to CO_2 enrichment is (for the period of interest) a monotonically increasing function of atmospheric CO_2 concentrations in the AEZ model, CO_2 fertilization would further drive up the cereal production potential by 2–5% across the 20 GCM-RCP combinations. This gives a total increase of cereal production potential by some 125.3 (±54.4) Mt and 179.6 (±52.5) Mt at the current and modernized irrigation efficiency rate, respectively, in comparison to the baseline.

Table 1. Transition matrixes of multi-cropping class extents (in Mha) between the baseline and the 2050s ensemble of 20 GCM-RCP simulations.

		Ensemble mean in the 2050							
		Limited single	**Single**	**Limited double**	**Double**	**Double with rice**	**Limited triple**	**Triple**	**Triple rice**	**Total (1981–2010)**
Irrigated cropland										
Baseline (1981–2010)	Limited single	**0.18 (0.05)**	0.20* (0.05)							0.38
	Single		**4.11 (1.49)**	5.38* (1.28)	0.14 (0.34)					9.63
	Limited double			**2.26 (1.07)**	2.90* (0.68)	0.42 (0.46)				6.64
	Double				**1.66 (1.43)**	6.46* (1.43)	0.80 (1.36)	0.08 (0.02)		9.00
	Double with rice					**3.37 (2.05)**	7.62* (1.12)	1.89 (1.36)		12.88
	Limited triple						**2.73 (1.90)**	7.30* (1.12)	0.05 (1.65)	10.08
	Triple							**5.02 (1.90)**	2.60 (1.83)	7.62
	Triple rice								**3.71 (1.45)**	3.71
	Total (the 2050s)	0.18	4.31	7.64	4.60	10.25	11.15	14.29	6.36	59.94
Rain-fed cropland										
	Limited single	**1.24 (0.09)**	0.70* (0.09)		0.07 (0.26)	0.90* (0.18)	0.06* (0.11)			1.97
	Single	0.07 (0.28)	**25.2 (1.74)**	5.73* (1.41)	1.39* (0.16)	1.69* (0.18)	0.58* (0.18)	0.09 (0.08)		31.03
	Limited double		0.72* (0.31)	**4.01 (0.27)**	**0.77 (0.26)**	**1.53 (0.57)**	2.77* (0.41)	1.52* (0.71)		7.08
	Double			0.32 (0.30)	0.65* (0.32)	0.64 (0.65)	**2.57 (0.74)**	4.67* (1.15)	0.05 (0.03)	8.33
	Double with rice			0.11 (0.00)	0.40 (0.28)	0.39 (0.46)	0.73* (0.32)	**3.59 (0.97)**	1.59* (0.55)	6.39
	Limited triple				0.09 (0.21)	0.12 (0.16)	0.20 (0.22)	0.31 (0.23)	**0.41 (0.14)**	1.04
	Triple						6.91	10.18	2.09	65.87
	Triple rice									
	Total (the 2050s)	1.31	26.58	10.17	3.37	5.27				

Notes: Standard deviations are in parentheses. The asterisk-marked mean values off-diagonal are significant at the 5% level.

Discussion

Our simulation experiments with the extended AEZ model revealed the significant increases in multi-cropping opportunities from the baseline (1981–2010) to the 2050s (2041–2070) in China. These newly available opportunities would be able to boost the total cereal production potential and 66% utilization of the increased potential under the condition of achieving the modernized irrigation efficiency rate by the 2050s would add 94.4 (±30.6) Mt cereal to China's total food supply in the 2050s. This amount, which is equivalent to 144.4% (±46.8%) of China's cereal imports and 14.9% (±4.8%) of China's cereal production in 2021, will be able to safeguard China's food security and ease the pressure on the global food market in the future.

This attractive prospect calls for technological and policy preparedness so that any newly emerging multi-cropping opportunities can be readily utilized in the decades to come. As irrigated cropland accounts for half of China's total cropland and produces more than 70% of China's current food production, securing future irrigation water supplies and more importantly, improving irrigation water use efficiency will be essential for exploiting future enhanced temperature regimes especially in north and northeast China.

The significant northward extensions of single-, double-, and triple-cropping zones would provide new opportunities for increasing production resilience to adverse climate conditions in the future. It has been increasingly recognized that crop-rotation with more varieties, including both cereals and non-cereals, is able to reduce risks from climate change related threats (21–25). For example, one of very recent studies (22) compared maize monoculture or maize-soybean rotation against rotations with more cereals and non-cereals at 11 long-term field trials across North America with 347 site-years of yield and climatic data to evaluate the impact of various crop rotations on yield resilience to adverse weather conditions. The results showed that rotations with more varieties of crops improved maize yields by 22.6% when the growing season conditions were good, and under drought conditions, maize yield losses were reduced by 14.0–89.9%, compared to a simple rotation. Another study (25), which was based on 18-year field experiment at an experimental farm in Canada, showed that the inclusion of cereal crops in rotations with soybean increases soybean yields and soil health, and compared with soybean monoculture, soybean yields were 39–44% higher for 2-year rotations with maize and wheat.

Despite the agronomic attractiveness of the increasing opportunities for multiple cropping and crop-rotation-based adaptation, it is worth noting that observed recent trends in southeastern and southern China have shown decreasing actual multi-cropping ratios, primarily driven by economic reasoning such as increasing labor costs and ample income earning opportunities outside agriculture. On one hand, the migration of rural labor force to non-farming activities has led to significant increase in the opportunity cost of labor input into farming activities. On the other hand, the dominance of smallholder farmland property-right arrangement bundled with the rigid *Hukou* system of household registration makes it very difficult to increase the labor productivity of farmers via land consolidation (26, 27). The *Hukou* system of household registration puts the Chinese population into rural and urban divisions and regulates the provision of essential social services in favor of households with urban *Hukou* (28). This context seems to suggest that it will be very challenging to reap the benefits of the emerging new multi-cropping opportunities in the future. Nevertheless, this would not present an

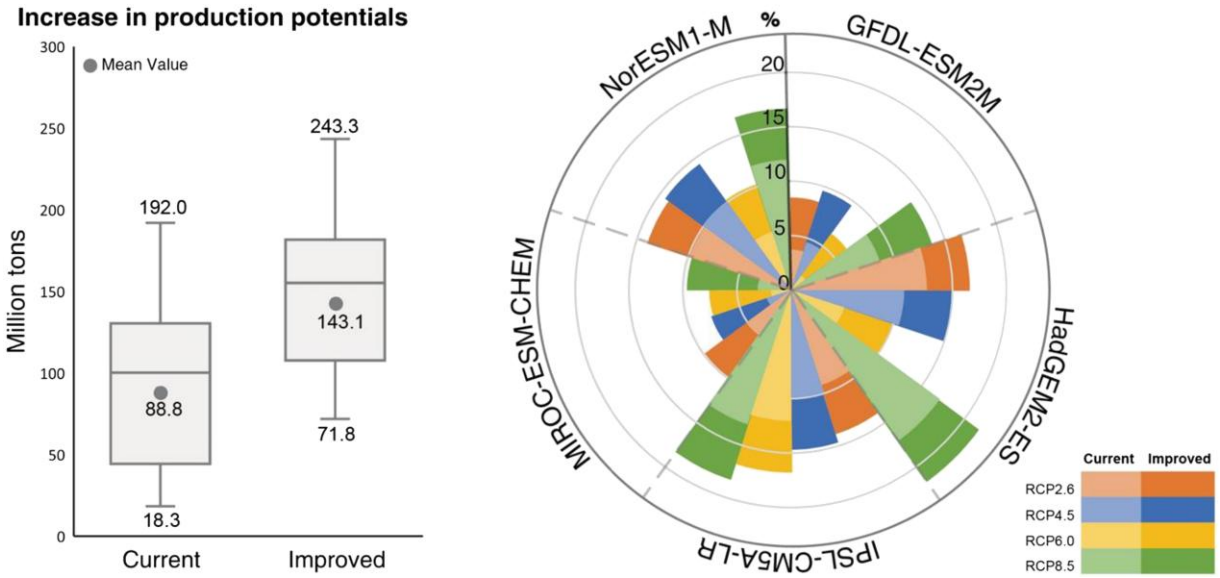

Fig. 2. Increases in the total grain production potentials from the baseline (1981–2010) to the 2050s (2041–2070) ensemble of 20 GCM-RCP simulations at the current ("Current") and the advanced ("Improved to 0.8") irrigation efficiency rate. Boxplots (left) show the distributions of the simulated increases in grain production potentials (in million tons) at the two irrigation efficiency rates, respectively. The Nightingale rose chart (right) presents the percentage share of the increase in the baseline production potential by GCM-RCP combination.

unsurmountable problem given the fact that China has successfully reformed state-ownership systems in the industrial and services sectors during the 1990s and 2000s (29).

In fact, China has implemented pilot land consolidation projects in almost all of China's provinces as presented in extended data Fig. 5 in (30). Based on China Land Consolidation and Rehabilitation (CLCR) data, China Rural Household Panel Survey (CRHPS) data, and high-resolution map of land-use, the analysis of Duan et al. (30) found that about 86% of croplands in China could be consolidated to establish a large-scale farming regime and this consolidation would reduce labor requirement by 39% and double income per laborer. It is because the consolidation would lead to an increase in knowledge exchange and machinery use by 59% and 91%, respectively, and a reduction in average cost by 50%. Another economics research (27) based on the same CLCR and CRHPS datasets revealed that farming income per laborer increases sharply with farm size, reaching the competitive level with non-agricultural workers at about 1.1 ha per farm. These two studies indicated that the decoupling of the *Hukou* system and the institutional arrangement of farmland property rights has been on the way and resulted in very encouraging results.

However, the most significant obstacle remaining is the lack of essential social services to immigrants who work in the urban sectors but keeping the rural *hukou* status (31, 32). A removal of this obstacle by radical reforms would make the livelihood of immigrant workers guaranteed in cities and as a result, they no longer need cropland to serve as a life insurance. The settle-down of existing immigrant workers and their families in cities would encourage more farmers to quit farming and move to urban areas permanently and this move would greatly facilitate the consolidation of farmland and the reduction in the number of farmers. In the countryside, it would become more likely that the remaining farmers will adopt modern technologies and climate change knowledge to boost profits associated with the increased farm size, and the increased multi-cropping and crop-rotation opportunities. At the national aggregation, the above constructive dynamics would be able to safeguard China's food security in the future.

Methods

The AEZ model

The AEZ model is designed to identify suitable agricultural land utilization options and estimate the corresponding crop production potentials at the grid-cell level across a large region (12). Since the early 1980s, the Food and Agriculture Organization of the United Nations (FAO) and the International Institute for Applied Systems Analysis (IIASA) have cooperated to develop and implement the AEZ modeling framework and databases. The model relies on the prevailing climate resources, soil profile and topography conditions, and detailed agronomic-based knowledge, and uses the standardized soil–plant–atmosphere interaction algorithms to simulate the biomass formation process of crop growth and soil water balance. The standardized soil–plant–atmosphere interaction algorithms make the AEZ well suited for evaluating suitability and production potentials of individual crop types under specific input and management conditions at the regional level where detailed and spatially explicit input data are relatively limited. As a result, it has been widely used to simulate crop suitability and productivity on each grid for the regional, national, and global assessment researches (26, 33–37). Both FAO and IIASA have been employing AEZ for evaluating land utilization potentials of natural resources in numerous assessments at global, regional, and national scales (12).

The agro-climatic elements of the AEZ model include key indicators and parameters of temperature, radiation, precipitation, and evapotranspiration, which condition the rates of net photosynthesis and allow plants to accumulate biomass and to accomplish the successive plant development stages. Data on climatic requirements of crop growth, development, and yield formation are also the basis for the multi-cropping suitability assessment because plants also have an obligatory development in time, which must be met if the photosynthetic assimilates are to be converted into economically useful yields of satisfactory quantity and quality. We refer to the above two sets of sorted and assembled indicators and parameters as the agro-climatic resource inventory.

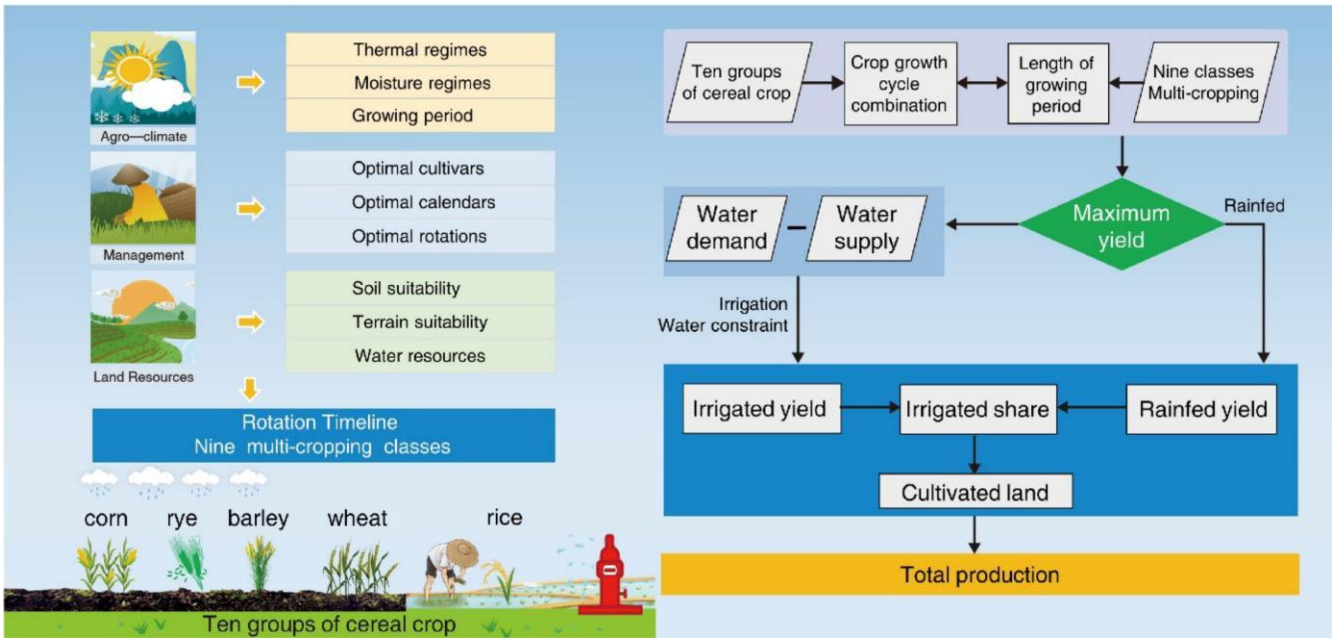

Fig. 3. The information flowchart of the production potential assessment under the irrigation water constraint.

When moisture conditions are met, the prevailing temperature regime determines crop performance. When temperature requirements are met, the growth of a crop is dependent on how well its growth cycle fits within the period when water is available, an agro-ecological concept known as the length of growing period (LGP). LGP provides an environmental characterization particularly relevant to the assessment of multi-cropping opportunities. It is defined as the number of days when mean daily temperature exceeds 5°C and soil moisture conditions are adequate for crop growth. Depending on the number of growing period days within a year, the LGP may be too short for cropping, may allow for one crop per year (e.g. in arid or dry semiarid tropics), or may permit the cultivation of a sequence of crops within one year (e.g. in humid tropics or subtropics). The AEZ methodology matches crop requirements with prevailing climate conditions in the following way: (i) compile crop adaptability inventory and define crop-specific temperature and moisture requirements; (ii) match crop temperature requirements with prevailing temperature regimes; (iii) determine optimal cropping calendar; and (iv) calculate crop-specific water deficits and estimate attainable yields within the optimal cropping calendar. The AEZ model runs over the whole time period at the daily time-step for the agro-climatic suitability and agro-ecological suitability analysis, which produce daily crop water balances and multiple cropping suitability maps. For the calculation of potential net biomass and yields, the AEZ model uses production functions which are based on eco-physiological principles, as presented on pages 213–215 in Ref. (12). A brief chart of information flows is presented in Fig. S2 and the detailed technical procedures of the multi-cropping suitability assessment are presented in Section SI-2-2.

Data

We worked with the latest GAEZ-v4. GAEZ-v4 applies bias-corrected climate data from the Intersectoral Impact Model Inter-comparison Project (ISI-MIP) (38, 39). ISI-MIP data at half-degree resolution and daily time-step include 20 combinations of five climate models (GFDL-ESM2M, HadGEM2-ES, IPSL-CM5A-LR, MIROC-ESM-CHEM, NorESM1-M) and four RCPs (RCP 2.6, 4.5, 6.0, and 8.5). GAEZ-v4 makes use of the Global Land Cover-SHARE (GLC-Share) database of FAO with spatial resolution of 30 arc-seconds, which incorporate the "best available" high-resolution land-use of China (12, 40). For compiling a spatial layer of irrigated land, we attribute the total extents of irrigated land reported in province-level statistics for 2010 to the spatial layer of cropland, distributing it according to irrigation ratios computed from 2010 county-level agricultural census data and giving priority to irrigated cultivation on paddy land and flat terrain. Soil attributes in GAEZ-v4 were derived from the Harmonized World Soil Database (HWSD v1.2) (41), which is a comprehensive and state-of-the art database developed by the IIASA and FAO. The HWSD has recently been recognized by the Global Soil Partnership as the best available global soil database at present. Data on climatic requirements of crops, their growth cycles, development stages, and yield formation periods were consolidated into the crops/land utilization types (LUTs) in GAEZ-v4.

The new module for sequential cropping choices and their production potentials

We added a new module to GAEZ-v4 model to identify the most desirable cropping sequence of cereal crops which would be able to produce the highest potential yield per unit of farmland. Fig. 3 depicts the information flowchart of this module. A brief introduction of its working steps is as follows.

In step one, by matching crop requirements with prevailing climate conditions as discussed above in the AEZ model subsection, a number of multiple cropping zones can be identified across grid-cells on map.

In step two, the module formulates the arrangement of crop sequence as a decision tree model. The structure of the decision tree is demonstrated in Fig. S3. The AEZ-China model of this study simulates the growth process and the best attainable yields of 120 crop varieties of 15 cereal crops (Table S1) on each grid-cell of farmland. Following the match procedure of step 1, these 15 crops are classified into five types, and every type has the long growth period (>120 days) varieties (without apostrophe mark in Fig. S3)

and short growth period (≤120 days) varieties (with apostrophe mark in Fig. S3). The objective function for optimizing the multiple cropping sequence is to maximize the best attainable yield per unit of farmland in the given grid-cell under rain-fed and irrigated condition, respectively. Mathematical formula of the objective function is as follows:

$$\text{Max } Q = \sum_{i,j,s} C_{i,j,s} \cdot X_{i,j,s}, \quad (1)$$

in which $X_{i,j,s}$ is the decision variable, which takes one when a decision is made to plant crop i, variety j, in season s, and zero otherwise. $C_{i,j,s}$ is the potential yield associated with the selection of $X_{i,j,s}$. The maximization procedure was run for rain-fed (Q_{RF}) and irrigated condition (Q_{IR}), respectively, at the grid-cell level.

In step three, we calculate maximum attainable water constraint production as weighted sum of production on rain-fed and irrigated cropland. The irrigation share of each grid-cell is calculated by Eq. (2), reflecting the specific water constraint of a location:

$$\text{IRS} = \frac{\text{WS}}{(ETm - P) \cdot A}, \quad (2)$$

where IRS stands for the share of irrigated land in the total farmland of the grid-cell, WS denotes water supply derived from the Water Resources Bulletin of China (13), $ETm - P$ represents water deficit from the gap between the specific crop water requirements (ETm) and precipitation (P), and A stands for total farmland area in the grid-cell.

WS is equal to the average water consumption of actual irrigation per hectare of cultivated land at the provincial level multiplied by the irrigation efficiency rate, both of which are provided in the Water Resources Bulletin (13). In the simulations for the 2050s, we do not consider the impact of climate change on irrigation water supply. However, we do consider the impact of increasing water use efficiency on water supply by assuming that the irrigation efficiency rate can be increased to the current level in developed countries. The reasons why we do not consider the impact of climate change on irrigation water supply are as follows: first, as explained in detail in Section SI-5, although the overextraction of groundwater had been a very severe issue in North China Plain before 2015 (37, 42, 43), both the national water management plan of China and very recent literature indicate a tendency of alleviation from 2015 onwards. Second, the currently best available predictions of future precipitation changes over China using a high-resolution regional climate model ensemble indicate that annual mean precipitation is likely to increase throughout the 21st century (0.078 mm/decade by the 2020s, 0.218 mm/decade by the 2050s, and 0.360 mm/decade by the 2080s), with some model results presenting a slightly decreased trend for certain regions (i.e. southeast) or seasons (i.e. autumn) in the 2020s (44). Therefore, we opted to assume that the current water supply level will not be significantly reduced by the 2050s.

The total potential production of cereals (Q) in the grid-cell is the weighted sum of the maximum potential production from multiple crops on irrigated and rain-fed farmland, using respectively shares IRS and (1 − *IRS*), as presented in Eq. (3).

$$Q = Q_{IR} \cdot \text{IRS} + Q_{RF} \cdot (1 - \text{IRS}). \quad (3)$$

Verification

To verify the reliability of the AEZ modeling procedures in identifying China's multi-cropping conditions, we compared the results of our assessment with data from remote sensing interpretation for the baseline period. Fig. 4 shows a very good agreement of simulated and observed data with regard to the north and northwest boundaries of the single-, double-, and triple-cropping areas. The major areas of each multi-cropping class/zone coincide well in the two sets of results. A more formal testing of the good agreement can be done by checking how the "population" of the multiple cropping grid-cells identified by remote sensing was distributed across the multiple cropping zones identified by the AEZ model simulation. Our remote sensing interpretation of the satellite images identified 36,415 simple-cropping, 38,850 double-cropping, and 3,236 triple-cropping grid-cells in total (see the last column of Table 2). We count how many of them fall into the single-, double-, and triple-cropping areas predicted by the AEZ model. The result shows that 2,131 (66%) of the 3,236 triple-cropping grid-cells fall into the AEZ's triple-cropping area, 38,694 (99.6%) of the 38,850 double-cropping grid-cells fall into the AEZ's double- and triple-cropping areas, and 36,247 (99.5%) of the 36,415 simple-cropping grid-cells fall into the AEZ's single-, double-, and triple-cropping areas (Table 2).

Please note that during the collective farming period (1956–1979) in China, maximizing the physical output of grain production (*yi liang wei gang*) has been the guideline of Chinese agricultural policy. As a result, the multiple cropping index for China as a whole had been increasing and reached the peak level of 152 in 1978, which was equal to about 96% of the best attainable level (45). During the period of 1979–1983, collective farming was gradually replaced by the household responsibility system (HRS). During the establishment of the HRS, increasing emphasis was given to market mechanism for guiding agricultural production decisions (31, 46), although central planning in the agricultural sector was still deemed essential. As a consequence, the multiple cropping index declined from the peak of 151–152 in 1978 to 147 in 1984 and the decline mainly took place in the triple- and then double-cropping areas of southern China (45–47). These dynamics have two important implications for our research. First, employing the earliest available remote sensing images of 1982–1986 from satellite Pathfinder is justified because the multiple cropping level during this transition period had not yet departed far away from the peak level in 1978, thus closer to the best attainable level as simulated by the AEZ model than those in later years. Second, it is reasonable that a relatively small number of single cropping grid-cells identified by remote sensing appeared in the AEZ's double-cropping (12,954, 35.57%) and triple-cropping (346, 0.95%) areas, and that a relatively small number of double-cropping grid-cells identified by remote sensing appeared in the AEZ's triple-cropping (9,625, 24.77%) areas.

It is also worth noting that the sequential cropping combinations in our AEZ assessment for the multiple cropping suitability give the priority to grain crops (Sections S-2-2 and S-3). By contrast, deriving multiple cropping patterns from remote sensing data has to take the existing crops in the field as given and some of the existing crops are cash crops such as winter rapeseeds rather than grain crops. This difference may explain why only 2,131 (66%) of the 3,236 triple-cropping grid-cells fall into the AEZ's triple-cropping area, because winter rapeseeds and other winter cash crops are popular in south Henan, Anhui, and Hubei provinces, which typically do not compete with grain crops for growing periods (26) and can be captured by remote sensing but ignored in the AEZ modeling.

For our analysis, the remote sensing interpretations of multi-cropping were extracted from 10-day composite AVHRR/NDVI time series images on an 8 × 8 km grid according to established

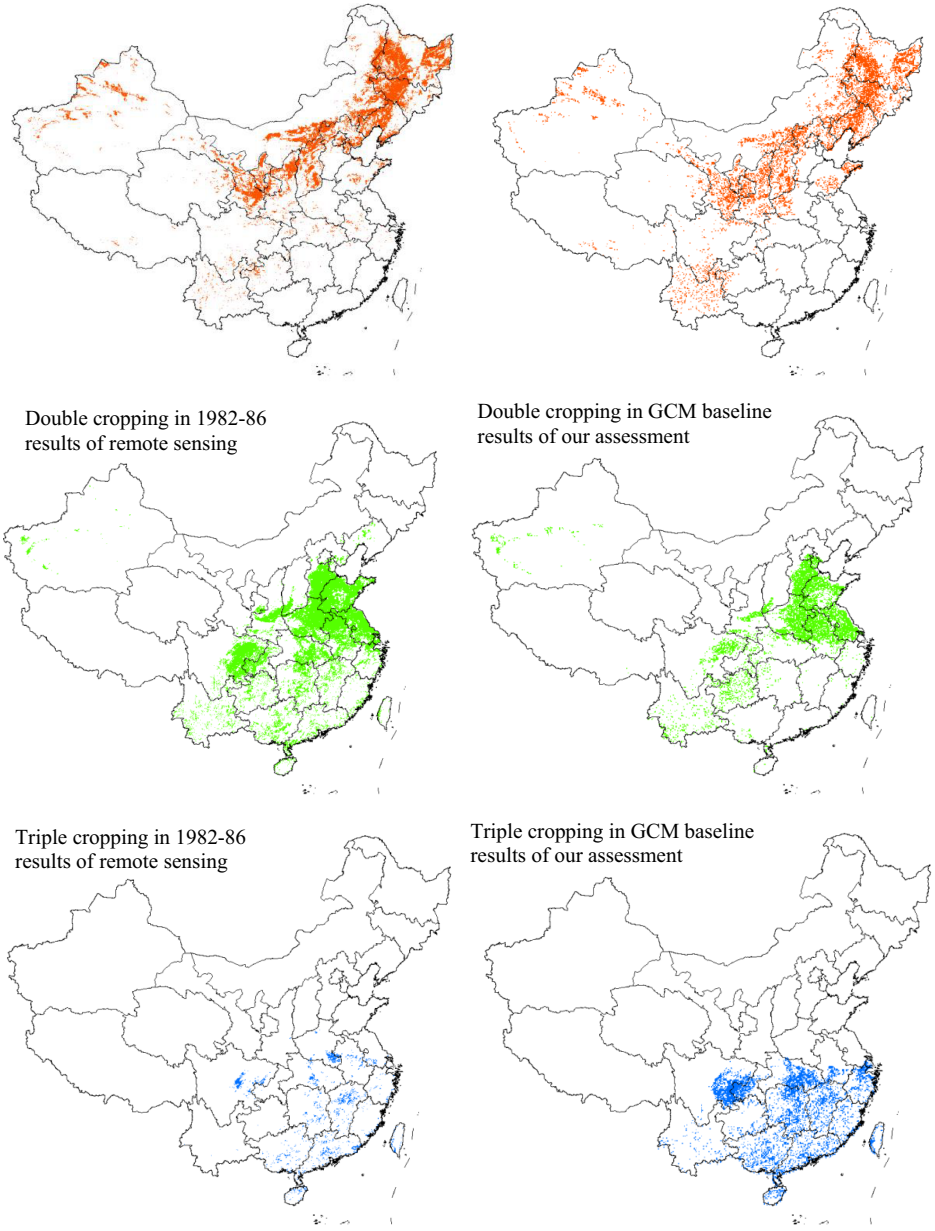

Fig. 4. Comparison of multi-cropping areas from remote sensing and our suitability assessment. The remote sensing results are for 1982–1986 and the suitability assessment results are for the baseline climate of 1981–2010. Multi-cropping areas from our assessment are calculated based on an area-weighted sum of multiple cropping index in irrigated and rain-fed farmland at the grid-cell level.

Table 2. Distribution of the number of multiple cropping grid-cells identified by remote sensing across the multiple cropping zones identified by the AEZ model simulation.

		AEZ's multiple cropping zones				
		No. cropping	**Single**	**Double**	**Triple**	**Total**
Identified by remote sensing	Single cropping	168	**22,947**	12,954	346	36,415
	Double-cropping	0	156	**29,069**	9,625	38,850
	Triple-cropping	0	0	1,103	**2,133**	3,236
	Total	168	23,103	43,126	12,104	78,501

phenological metrics and temporal features of farmland practices (see Section SI-3 and Fig. S4 for technical details). AVHRR refers to advanced very high resolution radiometer of the National Oceanic and Atmosphere Administration of the USA and NDVI stands for Normalized Difference Vegetation Index. AVHRR was put in operation in 1981 and its time series images are regarded as the only remote sensing source available for extracting comprehensive multi-cropping information for China over the period of 1981–

1999. The apparent consistency in terms of the spatial patterns and northern border lines of multi-cropping zones between the two sets of simulated and remote sensing derived results confirms the reliability of our method used to assess and delineate multi-cropping conditions.

Acknowledgments

We gratefully acknowledge the research partnership of IIASA in Austria and valuable advices from Mr. Harrij van Velthuizen. We thank Dr. Honglin Zhong, Mr. Yinghao Ji, Dr. Hanqing Xu, and Mr. Shaoxu Zheng for technical assistance.

Supplementary Material

Supplementary material is available at *PNAS Nexus* online.

Funding

This work was sponsored by the National Natural Science Foundation of China (Grant Nos. 41371110, 40921140410).

Author Contributions

Z.L., L.S., and Z.T. designed the research. Z.L., L.S., Z.T. G.F., and H.Y. contributed to the acquisition, analysis, and interpretation of data. Z.L., L.S., and Z.T. preformed the research. Z.L., L.S., and Z.T. led the drafting of the manuscript. Z.L., L.S., Z.T. G.F., and H.Y. contributed to the final writing of the article.

Data Availability

Bias-corrected climate data are published by the ISI-MIP (39). The GLC-Share database was published by the UN-FAO (40) and was built in GAEZ-v4 (12). HWSD v1.2 was published by UN-FAO and IIASA (41). Data on climatic requirements of crops, their growth cycles, development stages, and yield formation periods were consolidated into the crops/LUTs in GAEZ-v4 (12).

References

1 Waha K, *et al.* 2020. Multiple cropping systems of the world and the potential for increasing cropping intensity. *Glob Environ Change*. 64:102131.
2 Ray DK, Foley JA. 2013. Increasing global crop harvest frequency: recent trends and future directions. *Environ Res Lett*. 8:044041.
3 Xu J, *et al.* 2021. Double cropping and cropland expansion boost grain production in Brazil. *Nat Food*. 2:264–273.
4 Yang X, *et al.* 2015. Potential benefits of climate change for crop productivity in China. *Agric For Meteorol*. 208:76–84.
5 Ojeda JJ, Caviglia OP, Agnusdei MG, Errecart PM. 2018. Forage yield, water- and solar radiation-productivities of perennial pastures and annual crops sequences in the south-eastern Pampas of Argentina. *Field Crops Res*. 221:19–31.
6 Damien A, Isabelle T, Christovam B, Nicolas J, Vincent D. 2017. Land use sustainability on the South-Eastern Amazon agricultural frontier: recent progress and the challenges ahead. *Appl Geogr*. 80:86–97.
7 Ladha JK, *et al.* 2003. How extensive are yield declines in long-term rice-wheat experiments in Asia? *Field Crops Res*. 81:159–180.
8 Timsina J, Connor DJ. 2001. Productivity and management of rice-wheat cropping systems: issues and challenges. *Field Crops Res*. 69:93–132.
9 Liu L, Xu X, Zhuang D, Chen X, Li S. 2013. Changes in the potential multiple cropping system in response to climate change in China from 1960–2010. *PLoS One*. 8(12):e80990.
10 Huang C, *et al.* 2020. What is the consensus from multiple conclusions of future crop yield changes affected by climate change in China? *Int J Environ Res Public Health*. 17:9241.
11 Tian Z, *et al.* 2015. Agriculture under climate change in China: mitigate the risks by grasping the emerging opportunities. *Hum Ecol Risk Asses Int J*. 21(5):1259–1276.
12 Fischer G, *et al.* 2021. *Global agro-ecological zones v4—model documentation*. Rome: FAO.
13 Ministry of Water Resources of China. 2020. *China water resources bulletin*. Beijing: China Water Resources Publishing House.
14 Wallace JS. 2000. Increasing agricultural water use efficiency to meet future food production. *Agric Ecosyst Environ*. 82(1–3): 105–119.
15 Wang H. 2019. Irrigation efficiency and water withdrawal in US agriculture. *Water Policy*. 21:768–786.
16 Zhang B, *et al.* 2022. Identifying opportunities to close yield gaps in China by use of certificated cultivars to estimate potential productivity. *Land Use Policy*. 117:106080.
17 Deng N, *et al.* 2019. Closing yield gaps for rice self-sufficiency in China. *Nat Commun*. 10:1725.
18 Ministry of Agriculture of China. 2022. The import and export of agricultural products in China in 2021. http://www.moa.gov.cn/ztzl/nybrl/rlxx/202201/t20220127_6387781.htm
19 National Bureau of Statistics of China. 2021. Bulletin on the national grain output in 2021. http://www.stats.gov.cn/english/PressRelease/202112/t20211207_1825086.html
20 Ebi KL, Loladze I. 2019. Elevated atmospheric CO_2 concentrations and climate change will affect our food's quality and quantity. *Lancet Planet Health*. 3(7):E283–E284.
21 Renard D, Tilman D. 2019. National food production stabilized by crop diversity. *Nature*. 571:257–260.
22 Bowles TM, *et al.* 2020. Long-term evidence shows that crop-rotation diversification increases agricultural resilience to adverse growing conditions in North America. *One Earth*. 2: 284–293.
23 Yu T, *et al.* 2022. Benefits of crop rotation on climate resilience and its prospects in China. *Agronomy*. 12:436.
24 Xiao H, *et al.* 2022. Crop rotational diversity influences wheat–maize production through soil legacy effects in the North China Plain. *Int J Plant Prod*. 16:415–427.
25 Agomoh IV, Drury CF, Yang XM, Phillips LA, Reynolds WD. 2021. Crop rotation enhances soybean yields and soil health indicators. *Soil Sci Soc Am J*. 85:1185–1195.
26 Tian Z, *et al.* 2021. The potential contribution of growing rapeseed in winter fallow fields across Yangtze River Basin to energy and food security in China. *Resour Conserv Recycling*. 164:105159.
27 Wu Y, *et al.* 2018. Policy distortions, farm size, and the overuse of agricultural chemicals in China. *Proc Natl Acad Sci U S A*. 115: 7010–7015.
28 Chan KW, Zhang L. 1999. The "hukou" system and rural-urban migration in China: processes and changes. *China Q*. 160:818–855.
29 Qian Y. 2017. *How reform worked in China: the transition from plan to market*. Cambridge, MA: The MIT Press.
30 Duan J, *et al.* 2021. Consolidation of agricultural land can contribute to agricultural sustainability in China. *Nat Food*. 2:1014–1022.
31 Lu H, Xie H, He Y, Wu Z, Zhang X. 2018. Assessing the impacts of land fragmentation and plot size on yields and costs: a translog production model and cost function approach. *Agric Syst*. 161: 81–88.

32 Wang S, *et al.* 2021. Urbanization can benefit agricultural production with large-scale farming in China. *Nat Food*. 2:183–191.

33 Tubiello F, Fischer G. 2007. Reducing climate change impacts on agriculture: global and regional effects of mitigation, 2000–2080. *Technol Forecast Soc Chang*. 74(7):1030–1056.

34 Gohari A, *et al.* 2013. Climate change impacts on crop production in Iran's Zayandeh-Rud River Basin. *Sci Total Environ*. 442: 405–419.

35 Tian Z, *et al.* 2014. Improving performance of agro-ecological zone (AEZ) modeling by cross-scale model coupling: an application to Japonica rice production in Northeast China. *Ecol Modell*. 290:155–164.

36 Pirker J, Mosnier A, Kraxner F, Havlík P, Obersteiner M. 2016. What are the limits to oil palm expansion? *Glob Environ Change*. 40:73–81.

37 Zhong H, Sun L, Fischer G, Tian Z, Liang Z. 2019. Optimizing regional cropping systems with a dynamic adaptation strategy for water sustainable agriculture in the Hebei Plain. *Agric Syst*. 173:94–106.

38 Hempel S, Frieler K, Warszawski L, Schewe J, Piontek F. 2013. A trend-preserving bias correction—the ISI-MIP approach. *Earth Syst Dyn*. 4(2):219–236.

39 Warszawski L, *et al.* 2014. The inter-sectoral impact model intercomparison project (ISI–MIP): project framework. *Proc Natl Acad Sci U S A*. 111(9):3228–3232.

40 Latham J, Cumani R, Rosati I, Bloise M. 2014. *Global land cover SHARE (GLC-share) database beta-release version 1.0*. Rome: Food and Agriculture Organization of the United Nations. 40 p. (also available at http://www.fao.org/uploads/media/glc-share-doc.pdf).

41 Nachtergaele FO, van Velthuizen H, Verelst L, Wiberg D. 2012. *Harmonized world soil database (version 1.2)*. Rome: Food and Agriculture Organization of the United Nations (FAO), International Institute for Applied Systems Analysis (IIASA), ISRIC-World Soil Information, Institute of Soil Science—Chinese Academy of Sciences (ISSCAS), Joint Research Centre of the Europe. 50 p. (also available at http://www.fao.org/soils-portal/data-hub/soil-maps-and-databases/harmonized-world-soil-database-v12/en/).

42 Zhong H, *et al.* 2017. Mission impossible? Maintaining regional grain production level and recovering local groundwater table by cropping system adaptation across the North China plain. *Agric Water Manage*. 193:1–12.

43 Yang H, *et al.* 2021. Evolution of groundwater level in the North China Plain in the past 40 years and suggestions on its overexploitation treatment. *Geol China*. 48(4):1142–1155 (in Chinese with English abstract).

44 Guo J, Huang G, Wang X, Lin Q. 2017. Investigating future precipitation changes over China through a high-resolution regional climate model ensemble. *Earth's Future*. 5:285–303.

45 Walker KR. 1988. Trends in crop production, 1978–86. *China Q*. 116:592–633.

46 Albersen P, Fischer G, Keyzer M, Sun L. 2002. Towards estimating agricultural production relations for China. In: Song L, editor. *Dilemmas of China's growth in the twenty-first century*. Canberra: Asia Pacific Press. p. 135–175 (Chapter 9).

47 Lin JY. 1997. The role of agriculture in the transition process in China. In: Kydd J, Davidova S, Mackay M, Mech T, editors. *The role of agriculture in the transition process towards a market economy*. New York: United Nations. p. 63–75.